High Speed Operation Tests of Resolver Using AURIX Microcontroller Interface

M. Kozovsky * **P. Blaha** **

Brno University of Technology
Central European Institute of Technology
Purkynova 123
Brno 612 00, CZECH REPUBLIC

* *Phone: +420 54114 9845*
(e-mail:matus.kozovsky@ceitec.vutbr.cz)
** *Phone: +420 54114 6427*
(e-mail:petr.blaha@ceitec.vutbr.cz)

Abstract: This paper demonstrates possibility to use microcontroller AURIX TC277 interfaces for resolver signal processing and also for its carrier signal generation. Resolver support is integrated in Delta-Sigma analog to digital converter module. This module also contains resolver carrier signal generation. The paper also describes needed configuration and achieved results for the electrical speeds up to 80 krpm. Measured resolver position is compared with encoder position which is taken as a reference. The results from real experiments on a prepared hardware setup are also contained. The steps needed to achieve good compensation and correspondence between both sensors are detailed.

Keywords: Resolver, variable reluctance, encoder, incremental encoder, high speed sensing.

1. INTRODUCTION

Position (angle) sensors are widely used in many different applications. Especially in motor control applications, position sensors play very important role. They are required as feedback for precise positioning and they are also used for field oriented control (FOC) of AC motors to reach the optimal performance. Halder et al. (2016). Sensorless methods are also frequently used Akyol and Soylemez (2017), however sensorless control is difficult achievable for whole operation range.

Position sensors can be subdivided into two large categories, relative ones and absolute ones. Relative position sensors are able to recognise position difference, however they requires homing or alignment operation after the start-up.

Absolute position sensors are more suitable for Permanent Magnet Synchronous (PMS) motors because they do not require motor alignment during the start-up. Control algorithm for the motor is typically computed by the microcontroller of the inverter Bhadra and Patangia (2015); Samman et al. (2014).

These microcontrollers use sensors to measure motor currents, voltages and also position and speed of the motor. Measured data are processed and new Pulse Width Modulation (PWM) duties are calculated and send to the power stage using communication channel or they are used in microcontroller PWM module.

High integration leads to decreased number of integrated circuits and increased functionality of individual chips. Limiting integrating circuit count leads to decreasing product prices. The final product reliability is also higher. Preferred solution is to use sensors with analogue outputs and analogue to digital converters (ADC) of the microcontroller. This paper is focused on position sensor interface, especially to processing resolver signals.

The resolver is standard and widely used absolute position sensor. Many integrated circuits are available to process resolver signals, to convert them into encoder signals or to demodulate sin cos signals. These circuits have good precision and they are often configurable according to the resolver type and user requirements. Some resolver to digital converters use communication bus. Communication errors can occurs using such a bus. Time synchronization can be also problematic part in communication. High integration level of microcontrollers enables to include resolver signal processing directly in their modules. This leads to reducing the number of integrated circuits, to improved reliability and also to space savings.

The paper is organized as follows. After the introduction, resolver principle is summarized in second chapter. The third chapter describes test setup. Next chapter deals with resolver precision verification for three different rotational speeds. Fifth chapter concludes the achieved results.

2. RESOLVER PRINCIPLE

The resolver is typically used to measure absolute rotation angle by evaluating the signals from two sensing coils. These coils are excited by resolvers primary coil. Mutual inductances between primary coil and sensing coils are function of actual rotor position. Resolvers can be divided into two categories.

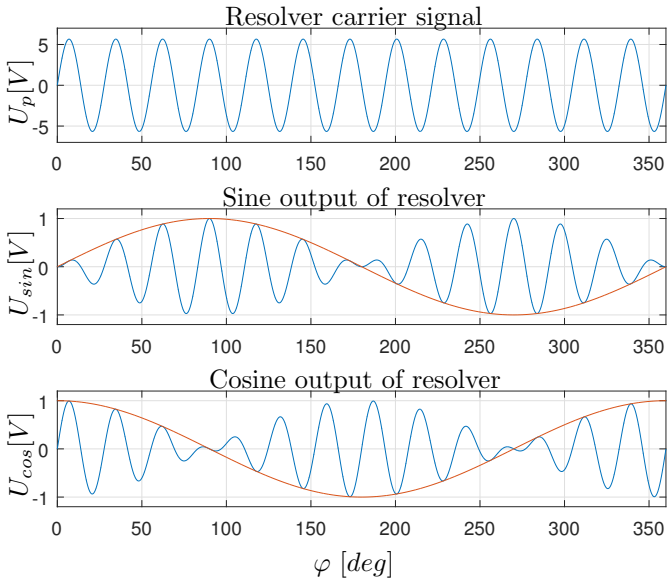

Fig. 1. Ideal resolvers signals

First category, classical resolver, consists of the primary excitation coil placed in rotor and two orthogonally placed coils in the stator. Primary coil is typically powered via rotary transformer (RT) or brushes, see Alipour-Sarabi et al. (2017).

Second category uses variable reluctance principle. Resolvers with variable reluctance do not need additional mechanism to power primary coil, because primary coil is located in stator along with sensing coils and can be directly connected to power source. Mutual inductances between primary and sensing coils depend on actual rotor position. Resolvers can be also constructed for multiple pole-pairs motors. This type of resolver measures absolute electrical position instead of mechanical position. Several sine and cosine signals are generated per one mechanical revolution, see Shi et al. (2017). Equations (1) describe the resolver behaviour.

$$\begin{aligned} U_p &= \frac{\mathrm{d}L_p i_p}{\mathrm{d}t} + \frac{\mathrm{d}M_{sin} i_{sin}}{\mathrm{d}t} + \frac{\mathrm{d}M_{cos} i_{cos}}{\mathrm{d}t} \\ U_{sin} &= \frac{\mathrm{d}M_{sin} i_p}{\mathrm{d}t} + \frac{\mathrm{d}L_{sin} i_{sin}}{\mathrm{d}t} \\ U_{cos} &= \frac{\mathrm{d}M_{cos} i_p}{\mathrm{d}t} + \frac{\mathrm{d}L_{cos} i_{cos}}{\mathrm{d}t} \end{aligned} \tag{1}$$

Variable U_P represents voltage connected to primary coil. Variables L_P, L_{sin} and L_{cos} are distributed inductances of individual coils. Mutual inductance between two sensing coils is zero because of their orthogonal placement. Variables M_{sin} and M_{cos} are mutual inductances between exciting coil and sensing coils. These inductances depend on absolute rotor position, so signal amplitude induced to sensing coils depends on absolute position too. Sensing coil current can be neglected because the voltage signal is connected to high impedance analog to digital inputs. The equations can be simplified into following form (2) using this hypothesis

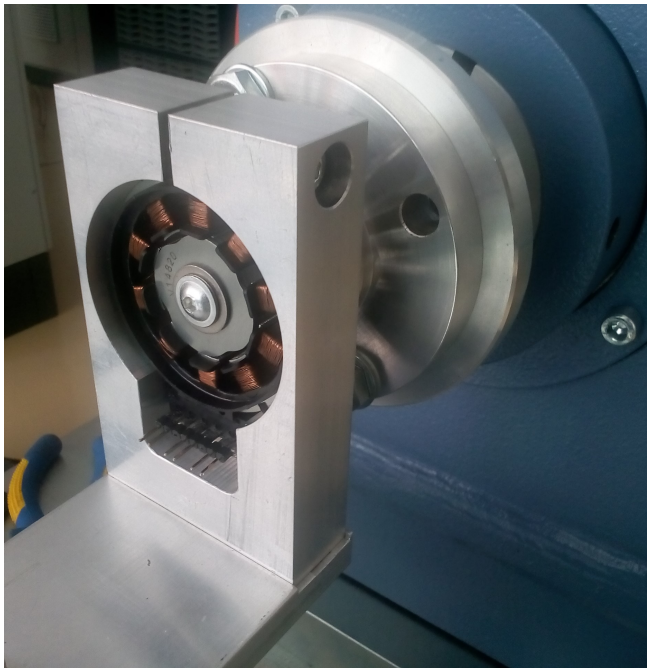

Fig. 2. Resolver connection to the dynamometer

$$\begin{aligned} U_p &= \frac{\mathrm{d}L_p i_p}{\mathrm{d}t} \\ U_{sin} &= \frac{\mathrm{d}M_{sin} i_p}{\mathrm{d}t} \\ U_{cos} &= \frac{\mathrm{d}M_{cos} i_p}{\mathrm{d}t} \end{aligned} \tag{2}$$

where

$$\begin{aligned} M_{sin} &= \sin(x\varphi) \\ M_{cos} &= \cos(x\varphi) \end{aligned} \tag{3}$$

Variable x takes into account resolver mechanical construction. This mechanical construction can be customized for different motors with various number of pole pairs. Carrier signal is used to excite resolver primary coil. Ideal Output voltages and carrier signal are shown in Fig. 1.

3. USED HARDWARE SETUP

The testing system was composed of following parts (see Fig. 3). The dynamometer was used as an actuator. It uses encoder position sensor to provide speed control. Also resolver sensor and microcontroller board (HybridKIT from Infineon) were used for tests.

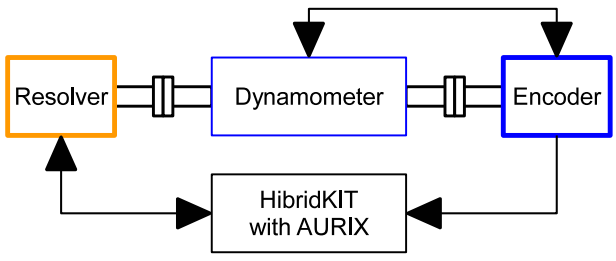

Fig. 3. Block diagram of used hardware

3.1 Variable Reluctance Resolver

Variable reluctance Tamagawa Singlesyn 4X-VRX resolver was used in the test. The mechanical construction of the resolver generates four sine and cosine signals per one mechanical turn.

This resolver type is suitable for PMS motors with four pole pairs. Absolute electrical position is directly measured instead of absolute mechanical position. Measured electrical speed is also four times higher than mechanical speed. Variable x for this encoder is $x = 4$.

Resolver carrier signal must have higher frequency than maximal rotating speed of measured object. This resolver type is constructed for 10 kHz excitation frequency.

3.2 Delta Sigma A/D Support for Resolver

Used AURIX microcontroller family has already integrated support for resolver connection. This additional feature is integrated in Delta-Sigma analog to digital converter (DSADC). The module is able to generate carrier signal for resolver primary coil.

Carrier signal is generated by microcontroller using PWM. Internal DSADC module clock signal is divided by user constant in programmable prescaler. This signal is subsequently used as PWM module clock. One carrier signal period consists of 32 steps. Each step equals a PWM period of 32 PWM clock cycles.

For example, microcontroller base frequency is 200 MHz and user prescaler is configured to 20. Carrier signal PWM module clock is 10 MHz. One PWM period uses 32 clock so one period of PWM takes 3.2 μs. Modulation frequency of carrier signal is 312.5 kHz in this case. The resulting frequency of carrier harmonic signal is 9.7656 kHz.

Several types of modulating signals can be selected. Triangle signal, rectangular signal or cosine signal are supported. The cosine signal is the most suitable one for the resolver.

Generated carrier signal must be power adapted and also higher frequencies caused by PWM must be filtered. PWM modulating frequency is 32 times higher in comparison with generated carrier signal. Excitation buffer circuit is used for filtering purposes. This circuit consists of operational amplifier and power transistors in output stage. The capacitor in feedback acts like a filter. The value of the capacitor must be adjusted to release the carrier signal and filter the PWM modulating frequency. Resistors in feedback adjust voltage level of carrier signal according to resolver specification.

Resolver sense coils signals are directly connected to the microcontroller. Two parallel Delta-sigma analog to digital converter inputs are used to provide conversion of both resolver signals at the same time. Time synchronization is essential for precise position measurement.

The resolver measured signals must be rectified so as to measure the magnitude of resolver signals properly. The carrier generator provides the sign information of the generated carrier signal for this purpose. The rectification of the received signals must be delayed to compensate the round trip delay through the system (driver, resolver coils, cables, etc.). For the rectification, the received values are multiplied with the delayed carrier sign signal. This synchronization is done for each channel separately to achieve the maximum possible amplitudes for each channel.

Time stamps are used to improve measured precision. Time stamps are realized using Timer Input Module (TIM). This module is part of Generic Timer Module (GTM). TIM module is able to detect and store time stamps of specific events. Actual time of free running timer base is copied into auxiliary registers upon an event. Precision of timer base is 10 ns. This module is configured to store times of two events. First event is start of PWM period. The same event starts current and voltages measurement procedure. Finished measurement starts motor control algorithms. Second time stamp is generated by DSADC result event. The internal structure of used modules can be seen in Fig. 4.

3.3 Processing Algorithms and Software

Available Infineon HybridKIT software framework was used as a background. All microcontroller interfaces for motor control and position measurement were initialized to guarantee the same behaviour as during active motor control. This program was properly modified to provide all necessary functionalities for testing. Simultaneous initialization of encoder and resolver position sensors was added.

Resolver carrier frequency was configured to 9.7656 kHz. This frequency is also used for DSADC sampling. Encoder mounted on dynamometer was used as position reference. The resolver was mounted to dynamometer instead of testing motor.

Both position sensors are mounted on one shaft. Absolute resolver precision declared by the producer is ± 2 electrical degrees. Mechanical connection to dynamometer can be seen in Fig. (2). Dynamometer is able to operate up to 20 krpm mechanical. Measured electrical speed is four times higher.

DSADC uses chain of selectable filters. Filter settings for both channels must be the same. Cascaded Integrator Comb (CIC) filters are used. These filters can be followed by other two Finite Impulse Response (FIR) filters. Overall time delay caused by this chain can be calculated using specific formulas which are provided by microcontroller producer. Time delays are also depended on actual filter configuration. Time delay of the whole measuring chain

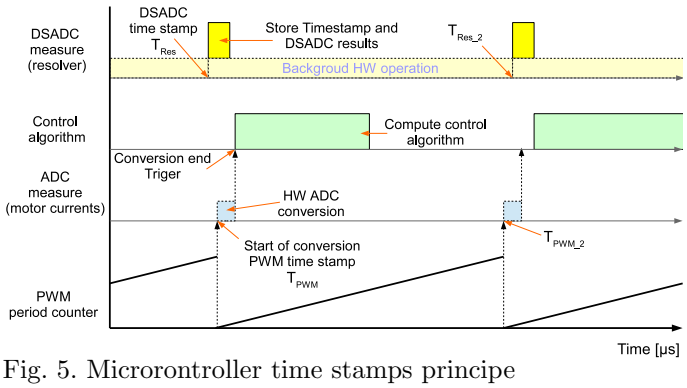

Fig. 5. Microrontroller time stamps principe

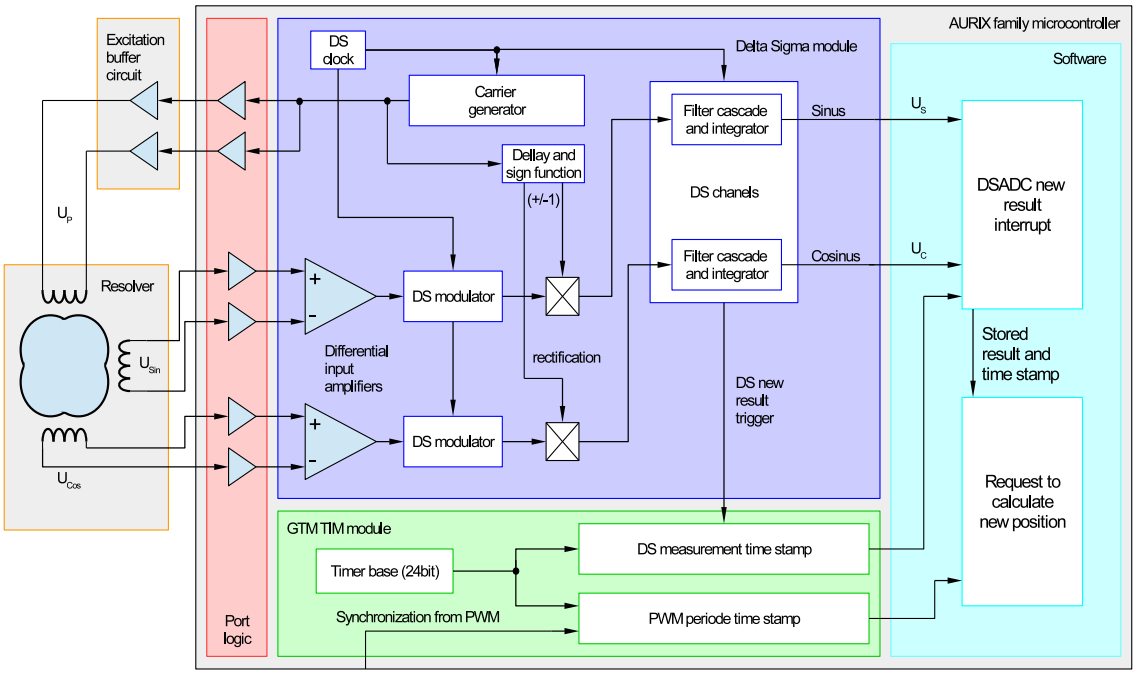

Fig. 4. Microcontroller internal structure and modules interconnection

needs to be calculated and compensated. This delay is approximately 102 μs. Compensation is realized using this time delay multiplied by actual speed of rotation. Resulting compensation angle is added to calculated angle.

Resolver angle measurement uses two software interrupts. First interrupt loads new measured values of DSADC and stores time stamp T_{Res} for following processing. Second interrupt is for control algorithm calculation. This interrupt is synchronized with PWM period, control algorithm can start after finished measurements of all control variables. Interrupt routines and other relevant microcontroller operations are shown in Fig. 5. Microcontroller calculates difference between last two time stamps. This time difference is multiplied by actual motor speed. Resulting angle difference is added to measured angle.

4. RESOLVER VERIFICATION

dSPACE DCI-GSI2 platform was used to monitor microcontroller variables in real-time. Sampling frequency of monitoring the variables was set to 10 kHz. This sampling frequency is same as motor PWM frequency. All measured signals and control algorithm are periodically calculated using the same sampling frequency.

First test was realised in a low speed, speed of dynamometer was configured to 500 rpm. Position of resolver and position of encoder were measured. The position difference between these two sensors was calculated. Measured precision of resolver sensor is lower in comparison to producer declared precision as Fig. 6 shows. Measured precision is approximately ± 2.5 electrical degree. However measured position error is periodic (one error period match to one electrical revolution). It follows that ripples are caused by not precise resolver mounting and not by analog measurement.

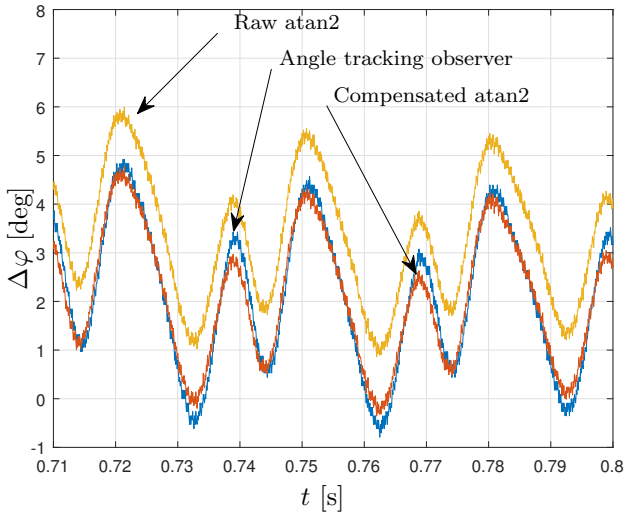

Fig. 6. Measured position difference to referenced encoder sensor at 500 rpm

Difference between raw position (yellow line in Fig. 6) and compensated position (red line in Fig. 6) is caused by added DSADC filters delay. This error represents approximately 1.2 electrical degrees (18 mechanical arcmin) at a speed of 500 rpm. Overall difference between reference encoder sensor position and compensated resolver position $\Delta\varphi$ is computed using following equation (5).

$$\Delta\varphi = \varphi_{enc} - \varphi_{res} + \varphi_{comp} \tag{4}$$

Variables φ_{enc} and φ_{res} represents actual positions of sensors. And φ_{comp} compensates the issue with misalignment of both sensors and with taking measurement in different time instants.

$$\varphi_{comp} = \varphi_0 + \omega_{el} \cdot T_{s_{dif}} \tag{5}$$

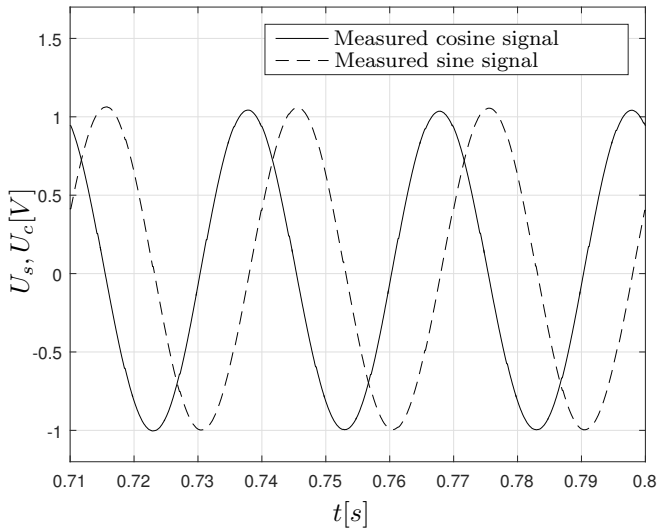

Fig. 7. Measured sine an cosine signals from delta sigma analog to digital converter module at a speed of 500 rpm

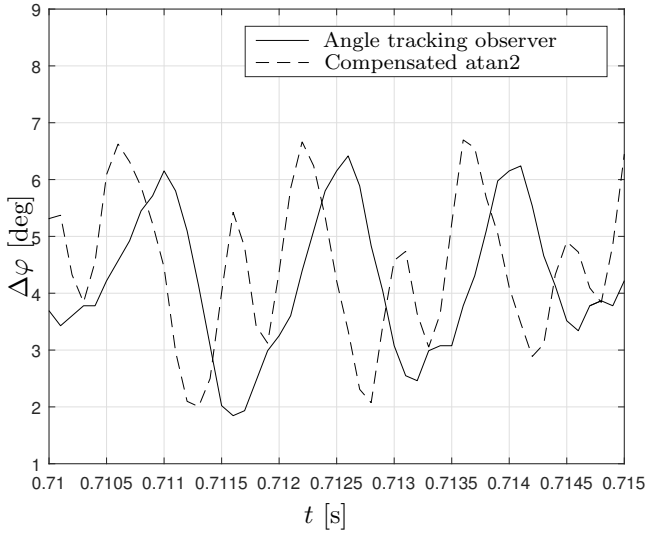

Fig. 8. Measured position difference to referenced encoder sensor at 10 krpm

Variable φ_0 represents the initial position difference caused by inaccurate initial position setting. This value was measured at low speed (500 rpm). Average position error difference value was used. Average value is more suitable because eliminates local extremes. Resulting measured position difference is about 2.1 electrical degree.

Second part of compensation is caused by microcontroller processing delay. This error is calculated from electrical speed ω_{el} and difference in sample times $T_{s_{dif}}$.

Resolver interface uses time stamps to calculate exact position in time of PWM update (end of every period). Encoder position is read from microcontroller registers during interrupt. This interrupt is delayed by additional analog measurements as Fig. 5 shows. This time should be constant for all speeds. Microcontroller program was prepared to measure this time difference between PWM update and encoder update event. Average value of the time difference is approximately 4 μs. $T_{s_{dif}}$ can be neglected for speed 500 rpm, so φ_0 is equal to measured position error.

Fig. 7 shows measured sine and cosine signals. These values are read directly from microcontroller DSADC result registers. Signals are not exactly centered. This deviation involve periodical position errors. Amplitudes of both signals are same. Measured signals can be simple corrected before position calculation. Amplitude, offset or signals orthogonality correction can improve final measured position and also speed.

Additional correction curve can be also used to improve position sensor precision. This method is suitable to improve precision of measured position and also precision of measured speed in final solution. The progresses of position and speed are also smoother using these additional methods.

Amplitude of measured signals is sufficient to proper position calculation.

Another measurement was realized at 10 krpm. Raw atan2 position calculation cannot be used for higher speeds, because position error without DSADC filter compensation is directly proportional to the actual speed. Uncompensated signals position error is 24 electrical degrees. Compensated signal position error for speed 10 krpm is approximately 4.4 electrical degrees.

Calculated sample difference for this speed using equation (5) is roughly 5 μs. Position oscillations in one electrical rotation shown by Fig. 6 are also visible in Fig. 8. Periodical position deviation follows from resolver construction itself or mechanical connection to dynamometer. These deviations cannot be caused by measurement or by microcontroller computation because one period of position inferences is equal to one electrical revolution.

Calculated 5 μs sample time error is more than measured microcontroller sample time difference measured by software itself. Difference between theoretical and real calculated sample times generate position error. Difference of 0.24 electrical degree will be caused by one microsecond deviation for speed of 10 krpm.

Last measurement was realised at speed of 20 krpm. Roughly only eight samples per one electrical revolution is measured for this mechanical speed. efective electrical speed is four times higher, so electrical speed is 80 krpm. Measured position error for this speed is about 6.75 electrical degree. Calculated sample difference $T_{s_{dif}}$ for this speed is the same as for 10 krpm. No additional error was detected during testing in comparison to 10 krpm speed. Measured position using angle tracking observer is smother in comparison to simple calculated position using only atan2 function and correction. Ripples of angle tracking observer position are ± 1.2 electrical degrees. Ripples of simple calculated position form Sine and Cosine signals are ± 2.5 electrical degrees. The value of ripples is the same for all speeds and can be caused by not precise resolver mounting as it was mentioned previously.

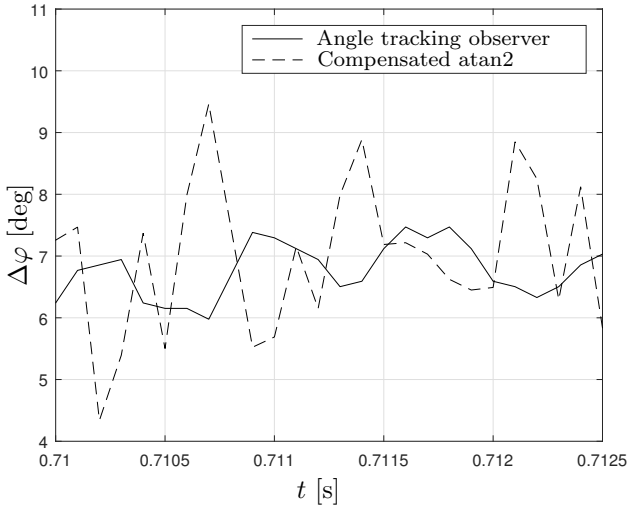

Fig. 9. Measured sine an cosine signals from delta sigma analog to digital converter module at a speed of 20 krpm

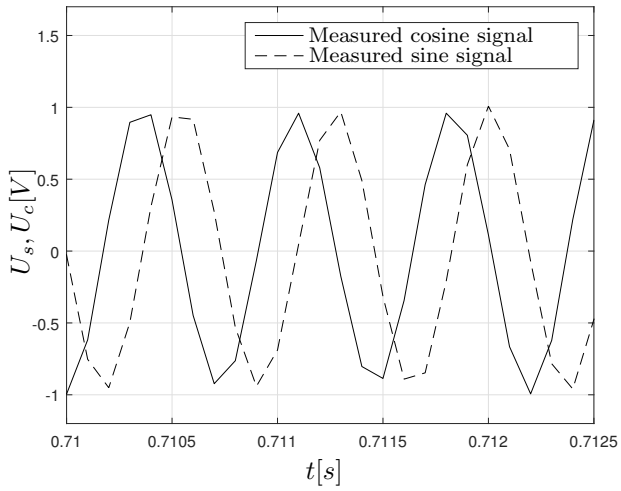

Fig. 10. Measured position difference to referenced encoder sensor at 20 krpm mechanic (80 krpm electrical)

Fig. 10 shows measured signals for 20 krpm. Amplitude of these signals is lower in comparison to amplitude from Fig. 7. However amplitude is also sufficient to correct position measurement. Tests also confirmed that used resolver and microcontroller interface can be used up to 80 krpm electrical.

5. CONCLUSION

Processing of high speed signals (up to 80 krpm electrical) was verified in this paper using AURIX microcontroller interfaces. This speed is being targeted in motor control applications in modern powertrains. The paper shows the ways how to compensate position measurements so as to fulfill the precision specified by resolver producer in the range from low speeds to high speeds up to 20 krpm.

The paper also demonstrates the possibility to use integrated solution of AURIX microcontroller family as an effective resolver to digital converter. This integrated solution has higher reliability in comparison to discrete solutions. Dynamics of filters and overall measurement queue can be configured according to physical dynamics of measured system. This configuration in conjunction with proper angle tracking observer dynamics can be adjusted for required application.

The bottleneck of the realized tests was inability to achieve perfect centering of the resolver parts. This problem is visible in obtained graphs and it can be further improved with additional compensation using look-up table.

ACKNOWLEDGEMENTS

The research was supported by ECSEL JU under the project 662192 3Ccar Integrated Components for Complexity Control in affordable electrified cars.

The completion of this paper was made possible by the grant No. FEKT-S-17-4234 - Industry 4.0 in automation and cybernetics financially supported by the Internal science fund of Brno University of Technology.

REFERENCES

Akyol, I.E. and Soylemez, M.T. (2017). Position Sensorless Field Oriented Control of IPMSM Under Parameter Uncertainties. *IFAC-PapersOnLine*, 50(1), 14501–14506. doi:10.1016/j.ifacol.2017.08.2301.

Alipour-Sarabi, R., Nasiri-Gheidari, Z., Tootoonchian, F., and Oraee, H. (2017). Performance Analysis of Concentrated Wound-Rotor Resolver for Its Applications in High Pole Number Permanent Magnet Motors. *IEEE Sensors Journal*, 17(23), 7877–7885. doi:10.1109/JSEN.2017.2761796. URL `http://ieeexplore.ieee.org/document/8063879/`.

Bhadra, S. and Patangia, H. (2015). A microcontroller based SHE inverter for maximum power point operation. In *2015 IEEE 11th International Conference on Power Electronics and Drive Systems*, 427–431. IEEE. doi:10.1109/PEDS.2015.7203552. URL `http://ieeexplore.ieee.org/document/7203552/`.

Halder, S., Agrawal, A., Agarwal, P., and Srivastava, S. (2016). Resolver based position estimation of vector controlled PMSM drive fed by matrix converter. In *2016 Second International Innovative Applications of Computational Intelligence on Power, Energy and Controls with their Impact on Humanity (CIPECH)*, 68–72. IEEE. doi:10.1109/CIPECH.2016.7918739. URL `http://ieeexplore.ieee.org/document/7918739/`.

Samman, F.A., Waris, T., Anugerah, T.D., and Mide, M.N.Z. (2014). Three-phase inverter using microcontroller for speed control application on induction motor. In *2014 Makassar International Conference on Electrical Engineering and Informatics (MICEEI)*, 28–32. IEEE. doi:10.1109/MICEEI.2014.7067304. URL `http://ieeexplore.ieee.org/document/7067304/`.

Shi, T., Hao, Y., Jiang, G., Wang, Z., and Xia, C. (2017). A Method of Resolver-to-Digital Conversion Based on Square Wave Excitation. *IEEE Transactions on Industrial Electronics*, 1–1. doi:10.1109/TIE.2017.2782228. URL `http://ieeexplore.ieee.org/document/8186205/`.